Water Science & Technology

Water Science & Technology Vol 89 No 5, 1297 doi: 10.2166/wst.2024.063

Evaluating water quality and fouling propensity in a pilot-scale ceramic membrane bioreactor treating municipal wastewater subjected to increasing salinity levels

Salaheddine Elmoutez [a,*], Hafida Ayyoub[b], Mohamed Chaker Necibi[a] and Mohamed Taky[b]

[a] International Water Research Institute IWRI, Mohammed VI Polytechnic University, Lot 660, Hay Moulay Rachid Ben Guerir 43150, Morocco
[b] Laboratory of Advanced Materials and Process Engineering, Faculty of Sciences, Ibn Tofail University, BP 1246, Kenitra, Morocco
*Corresponding author. E-mail: salaheddine.elmoutez@um6p.ma

SE, 0000-0002-7673-6677

ABSTRACT

This study aims to optimize the removal of carbon and nitrogen pollutants from saline municipal wastewater using both membrane-based and biological treatment methods. It examines a pilot-scale sequential aerobic ceramic membrane bioreactor (AeCMBR) under various salinity levels (0–20 g NaCl/L) to assess biological processes and fouling behavior. While high COD removal rates of (≈90%) were consistently achieved, ammoniacal nitrogen removal dropped from 82 to 55% at 15 g NaCl/L, despite increased oxygenation flow rates. Notably, the biomass quickly adapted to salinity changes. Indicators such as mixed liquor suspended solids (MLSS), mixed liquor suspended volatiles (MLVSS), MLVSS/MLSS ratio, and sludge volume index (SVI) showed no significant correlation with increasing salt concentrations. Soluble microbial product (SMP) production was also unaffected by rising salinity levels. The transmembrane pressure (TMP) fluctuated, with the most pronounced trend at 15 g NaCl/L, even after reducing the flux from 20 to 15 L/m^2/h. The primary fouling mechanism observed was reversible cake deposition. Overall, this research enhances our understanding of short-term operational impacts on AeCMBR performance as a function of different salinity levels.

Key words: aerobic membrane bioreactor, membrane fouling, municipal wastewater treatment, organic removal, salinity

HIGHLIGHTS

- We investigated an AeCMBR pilot plant-treated wastewater with rising salinity.
- Reversible cake deposition fouled the membrane consistently.
- Graduated salinity had no consistent impact on treatment efficiency.
- Nitrifiers can handle up to 15 g/L NaCl with proper aeration.
- Complex municipal wastewater needs thorough homogenization.
- The study offers valuable control and operation insights for practitioners.

GRAPHICAL ABSTRACT

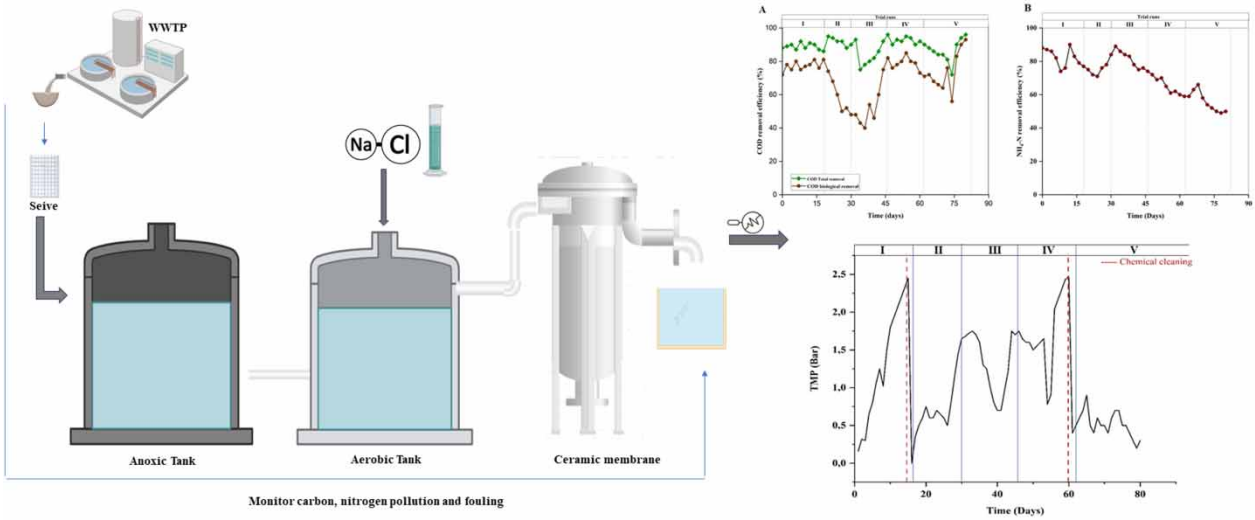

1. INTRODUCTION

Water scarcity poses a considerable obstacle to the sustainable development. Many industries, such as tanning, food processing, petrochemicals, and the use of seawater for wastewater flushing, generate substantial amounts of saline wastewater (SWW) (Zhang *et al.* 2014). In arid regions, particularly those near coastlines in Saharan regions, desalinated seawater is used for freshwater supply, resulting in municipal wastewater with elevated salt levels. SWW may represent as much as 5% of the total global effluent (Lefebvre *et al.* 2007).

SWW treatment can be treated through both physical and chemical methods. Nevertheless, physical–chemical treatment methods require substantial quantities of chemical reagents, significant energy input, and result in the generation of chemical-loaded sludge (Capodici *et al.* 2020). On the other hand, the biological processes are commonly employed for the treatment of domestic and industrial wastewater, as it is cost-effective and generates by-products that pose minimal risk to the environment (Luo *et al.* 2019). The objective of biological treatment systems is to create processes that not only meet regulatory requirements but also promote the growth of biological activity, including carbon oxidation, nitrification, and denitrification, in response to the increasing need for wastewater reuse (Capodici *et al.* 2020). Enhancing the performance of biological treatment systems for SWW involves prolonging the hydraulic retention time (HRT) (Wang *et al.* 2015), and augmenting the biomass within the reactors (Yu *et al.* 2011).

To address the challenges posed by salt content, researchers have explored innovative biological technologies for SWW treatment, including the membrane bioreactor (MBR) system. MBRs were proven effective in treating various types of wastewaters, including municipal and industrial effluents, polluted surface waters, and landfill leachates (Wintgens *et al.* 2005; El-Ghzizel *et al.* 2020; Elfilali *et al.* 2022; Zait *et al.* 2022). The utilization of MBR technology presents several notable advantages when compared to conventional activated sludge systems. These advantages include enhanced effluent quality, reduced spatial requirements, extended sludge retention time, nearly complete absence of pathogenic bacteria in the effluent, and accelerated biomass acclimatization (Judd 2010).

Polymeric membranes offer economic advantages over alternatives such as ceramic membranes (Elmoutez *et al.* 2023). However, the integration of inorganic membranes into MBRs facilitates a more direct and efficient capture of organic matter, with generally higher flux compared to polymeric membranes (Wenten *et al.* 2016). Ceramic membranes are strategically suitable for treating wastewater under extreme conditions, notably at an industrial scale, encompassing high temperature, pressure, salinity, and organic load (Wenten *et al.* 2016; Aryanti *et al.* 2020; Elmoutez *et al.* 2023). Ceramic membranes, mainly made from aluminum oxide, are well-suited for product clarification, particularly in the food industry (Aryanti *et al.* 2020). With a substantial pore size ranging from 0.05 to 0.5 μm, these membranes enable highly efficient filtration processes (Elmoutez *et al.* 2023). In a prior investigation, a semi-industrial ceramic microfiltration membrane clarified a maltodextrin feed solution at 90 °C, achieving high degrees of clarification. Employing ceramic membranes

resulted in noteworthy cost savings compared to alternative filtration methods. The study showed that, as well as improving maltodextrin clarification, the ceramic membrane saved USD 292,549 per year compared with rotary vacuum filtration (Aryanti *et al.* 2020).

MBRs can employ selective membranes to extract pollutants from wastewater via biomedias, leading to a highly specific sorption process for the biodegradation of toxic organic pollutants in wastewater from the chemical industry. Numerous studies indicate the successful removal of over 99% of various toxic organic compounds (e.g., 3-chlorobenzoate, 2,3-dichloroaniline, aniline, 2,4-dichlorophenol, 4-chloroaniline and benzene) using extractive membrane bioreactors (Wenten *et al.* 2020).

MBR integrates membrane technology with the activated sludge process, allowing for the preservation of a high biomass concentration. This biomass includes slow-growing autotrophic microbes, notably *ammonia-oxidizing bacteria (*AOB) (Chen & LaPara 2008).

Nonetheless, the presence of salt can inhibit microbial activity, causing phenomena such as plasmolysis and the impairment of enzyme function due to elevated osmotic pressure. These effects can lead to limited biological activity, and even the incapacitation of the biological system in MBRs (Luo *et al.* 2019).

Numerous studies have focused on biological treatment performances in MBRs for the treatment of SWW. Ayyoub *et al.* (2023) conducted a pilot-scale aerobic MBR study on fish canning wastewater, achieving impressive results including a 97% chemical oxygen demand (COD) removal rate, 98% biological oxygen demand (BOD), 90% nitrate, and over 97% removal rates for total Kjeldahl nitrogen (TKN) and total phosphorus (TP) (Ayyoub *et al.* 2023). Yogalakshmi & Joseph (2010) investigated the influence of NaCl shock loading on COD removal efficiency using a bench-scale submerged aerobic MBR. They maintained a steady-state organic loading rate (OLR) of 3.6 g-COD/L/d and an HRT of 8 h. Their feed biomass consisted of activated sludge, which underwent acclimatization for 30 days and was then exposed to synthetic wastewater. They achieved a COD removal efficiency of nearly 95% with NaCl shock loads ranging from 5 to 30 g/L. However, the efficiency dropped to 77 and 64% with shock loads of 50 and 60 g/L, respectively (Yogalakshmi & Joseph 2010). Ye *et al.* (2009) noted that salinity had a significant impact on nitrifying bacteria in a sequential batch reactor (SBR) (Ye *et al.* 2009). Furthermore, the impact of salinity on bacterial populations can lead to increased effluent turbidity, as demonstrated by Amin *et al.* (2014); Amin *et al.* 2014). Uygur (2006) reported a decline in NH_4-N removal efficiency, decreasing from 3.0 to 0.80 mg NH_4-N/g biomass/h, and a decrease in PO_4-P removal efficiency, decreasing from 0.36 to 0.08 mg PO_4-P/g biomass/h, as salt content increased from 0 to 6% in experiments involving an SBR (Uygur 2006). In a study conducted by Luo *et al.* (2015), the effects of salinity on biomass characteristics and membrane fouling in MBR systems were investigated. It was observed that ammonia removal efficiency significantly decreased at high salinities, especially right after salinity shock loading, indicating that autotrophic biomass is adversely affected by high-salinity environments (Luo *et al.* 2015). A hypersaline environment can result in the reduction or even disappearance of specific non-halophilic bacteria while favoring the dominance of halophilic microbes. This shift in microbial populations can have a significant impact on pollutants removal efficiency (Tan *et al.* 2019).

Jang *et al.* (2013) highlighted that reduced ammonia removal and increased membrane fouling in the treatment of high-salinity wastewater were attributed to specific characteristics of the microbial community. The presence of salt in wastewater can exacerbate membrane fouling by causing sludge deflocculation (Jang *et al.* 2013). Furthermore, alterations in the bacterial community composition may lead to changes in the production of soluble microbial products (SMPs). SMPs are organic substances released by microorganisms as part of their normal metabolic processes and during the decomposition of biomass in biological systems (Ni *et al.* 2011). These SMPs can contribute to the formation of a gel layer on the membrane surface (Ramesh *et al.* 2007) and are generally recognized as playing a pivotal role in membrane fouling (Teng *et al.* 2020).

Numerous research studies have primarily focused their investigations on high-strength or synthetic wastewater regarding exploitation of MBRs for SWW treatment. Nevertheless, there is a notable research gap, particularly concerning municipal wastewater treatment, due to its inherent complexity regarding dilution and composition. Furthermore, maintaining consistent feed conditions presents significant challenges. Thus, the primary objective of this study is to thoroughly analyze the immediate impacts resulting from the observed rise in salinity in municipal wastewater on the performance of the highly promising MBR technology for large scale applications. This comprehensive evaluation encompasses aspects such as carbon and nutrient removal, the evolution of SMPs, trends in membrane fouling, and the characteristics of settled sludge. The expected outcomes of this research extend beyond enhancing our understanding of system performance and biomass behavior; they are anticipated to make a substantial contribution to the advancement of more effective control methods for MBR utilized in the treatment of SWW.

2. MATERIALS AND METHODS

2.1. Experimental system and protocol

The aerobic ceramic membrane bioreactor (AeCMBR) pilot plant, located in the Laboratory of Advanced Materials and Process Engineering, University of Kenitra in Morocco (depicted in Figure 1), comprises various components. This system is equipped with a 200-L high-density polyethylene feed tank. It serves as both a buffer tank and a feed source, and us used to add salt before conveying it to the pilot system. The AeCMBR pilot unit, employing a pre-denitrification approach, is constructed with two sequential reactors: a 20-L anoxic reactor designed for denitrification and a 40-L oxidation reactor dedicated to nitrification. The oxidation reactor is equipped with four self-contained diffusers positioned at the tank's base, each individually controlled by a shut-off valve to precisely manage air introduction, regulated through a control valve. To facilitate the movement of wastewater from the storage tank to the reactors, a feed pump is employed. Meanwhile, the transfer of effluent from the anoxic tank to the aerobic reactor is managed by a peristaltic pump.

Furthermore, this pilot plant is equipped with an external ceramic ultrafiltration membrane characterized by the following specificities:

- module type: tubular P10,
- Filtration area: 0.45 m²,
- cut-off: 15 kDa (falling within the 10–20 nm range),
- membrane length: 1,178 mm
- channel diameter: 6 mm.

This configuration is designed to provide tangential filtration, with the suspension being filtered from the inside to the outside of the membrane. For the collection of permeate, a peristaltic pump, accompanied by a set of valves, is employed. The retentate is recycled to the nitrification reactor using a concentric tube heat exchanger and a back pressure valve. To maintain the membrane's cleanliness, a 20-L cleaning-in-place tank is positioned between the reactors and the membrane unit.

The influent wastewater, as well as the primary sludge used as an inoculum for this study, sourced from the municipal wastewater treatment plant in Kenitra. The collected wastewater was stored and homogenized (mechanically) before being introduced into the pilot system. Pertinent parameters of the municipal wastewater, including both mean and standard deviation values, are summarized in Table 1. To facilitate monitoring, the reactors were equipped with probes to track various parameters such as pH, dissolved oxygen, redox potential, and temperature. The measurements obtained from these probes were directly displayed on the electrical control panel.

The experiment was conducted in five distinct phases, as outlined in Table 2. Each phase was characterized by the introduction of varying doses of sodium chloride (NaCl). Phase I did not involve any salt addition, followed by Phase II (5 g NaCl/L), Phase III (10 g NaCl/L), Phase IV (15 g NaCl/L), and Phase V (20 g NaCl/L). Throughout the experiment, an HRT of 20 h was

Figure 1 | Configuration of the pilot-scale AeCMBR plant.

Table 1 | Influent municipal wastewater properties on average

Parameter	Value	SD
COD (mg/L)	683.65	60.46
BOD_5 (mg/L)	114	51.76
TSS (mg/L)	411	193.90
NH_4-N (mg/L)	82.66	26.58
NO_3^-	29.37	10.17
PO_4-P (mg/L)	5.57	3.61
pH	8.18	1.52
Conductivity (mS/cm)	16.46	12.11
Salinity (g/L)	3.68	2.52

SD, standard deviation; TSS, total suspended solids.

Table 2 | The operational conditions of the pilot-AeCMBR

Phases	Days	HRT (h)	SRT (day)	Dissolved oxygen (mg/L)	Oxygenation rate (NL/h)	Temperature (°C)	NaCl (g/L)	Permeate flux (LMH)
I	0–18	20	–	2(on)-4(off)	700–1,000	21.5	0	20
II	19–30	20	–	2(on)-4(off)	700–1,000	21.5	5	20
III	31–46	20	–	2(on)-4(off)	1,000–1,500	21.5	10	15
IV	47–62	20	–	2(on)-4(off)	1,000–1,500	21.5	15	15
V	63–80	20	–	2(on)-4(off)	1,000–1,500	21.5	20	15

maintained. This was crucial to ensure the acclimatization of the biomass to the increasing salinity levels, especially for sensitive nitrifying microorganisms like AOB and nitrite-oxidizing bacteria (NOB). The pilot plant operated for nearly three months without any sludge withdrawal, resulting in an undefined solids retention time (SRT). Dissolved oxygen levels inside the aerobic tank were consistently within a range of 2–4 mg/L. Oxygenation rates varied, ranging from 700 to 1,000 NL/h for the initial two phases and subsequently increased to a range of 1,000–1,500 NL/h for Phases III, IV, and V. Notably, the net membrane fluxes in the AeCMBR were kept constant during operational periods, with rates of 20 and 15 $L/m^2/h$ (LMH) for Phases I and II and Phases III, IV, and V, respectively.

2.2. Analytical tools and methods

The sampling plan involved collecting influent wastewater, mixed liquor, and permeate three times a week. Various parameters were monitored throughout the experiment, including total chemical oxygen demand (TCOD), which was measured using a Hach DR2800 spectrophotometer, and BOD over 5 days (BOD_5), determined using OxiTop WTW equipment. Total and volatile suspended solids (TSS and VSS), TKN, ammonium nitrogen (NH_4-N), nitrate nitrogen (NO_3-N), nitrite nitrogen (NO_2-N) were measured using an electrode (Sension MM 340). Phosphate phosphorus (PO_4-P) levels were assessed, and pH was measured with a JENWAY pH meter. Electrical conductivity was determined using a conductivity meter (inoLab). These measurements were conducted following standardized protocols outlined in APHA (2005) (WEF no date). Additionally, measurements of MLSS, MLVSS, and the sludge volumetric index (SVI) were carried out following established procedures. SMPs were periodically quantified using filtration methods (SMP concentrations in the AeCMBR supernatants were assessed by filtering them through cellulose acetate syringe filters with a pore size of 0.45 μm). To distinguish between the removal achieved through biological processes and that facilitated by membrane filtration, two separate removal efficiencies were calculated. The biological removal efficiency was determined based on the difference between influent TCOD and the measured COD in the supernatant of mixed liquor samples (COD_{SUP}). Conversely, the total COD removal efficiency was calculated by comparing influent TCOD and permeate TCOD.

2.3. Membrane cleaning

To continuously monitor reactor performance and control fouling, transmembrane pressure (TMP) was consistently recorded at 20-s intervals using computer-based systems. In cases of constant flux operation, an increase in fouling was directly associated with a rise in TMP. Pressure measurements were obtained through pressure transmitters and pressure gauges positioned at various points in the system, including just before the membrane module inlet, at the membrane module outlet, and within the permeate collection circuit. The pressure sensor recorded the pressure within the ultrafiltration module's permeate collection circuit, and this value was displayed on the control panel. The recorded measurement signals were also consistently logged in the programable automaton.

For the first time in the AeCMBR pilot, an intermittent filtration cycle was implemented. This cycle consisted of 13 min of suction followed by 2 min of relaxation (no suction). The purpose of this cycle was to strike a balance between effective membrane cleaning and preserving the overall filtration process efficiency. For cleaning purposes, tap water was sourced from the clean-in-place tank. The TMP threshold for suspending AeCMBR operations due to fouling ranged from 0.3 to 2.5 bar. Once this threshold was reached, a chemical cleaning process was initiated.

The chemical cleaning process involved the use of solutions with specific pH levels, namely NaOH (pH = 11) and H_2SO_4 (pH = 3). These solutions were introduced into the clean-in-place tank and then conveyed to the membrane via the filtration pump, with tap water acting as an intermediary before and after the chemical cleaning process. The combined application of these solutions and tap water spanned a duration of 1 h, aiming to restore the membrane to its initial permeability.

2.4. Membrane fouling monitoring

The investigation into specific fouling mechanisms delved into the application of the resistance-in-series model. To assess each resistance component, a modified version of the procedure initially proposed by Mannina *et al.* (2016) was employed (Mannina *et al.* 2016). Determination of the membrane resistance was achieved through the well-established Darcy Equation (1):

$$R = \frac{\mathrm{TMP}}{\mu J} \tag{1}$$

where J signifies the flux in $m^3/(m^2.\ s)$, TMP represents the transmembrane pressure in Pa, μ stands for the permeate viscosity in (Pa.s), and R denotes the membrane filtration resistance as 1/m.

For the AeCMBR pilot plant, a cyclic operational approach involving 13 min of filtration followed by 2 min of relaxation was implemented. During these relaxation periods, it was assumed that all reversible fouling was eliminated, creating a robust shear effect during backwashing. Under each specific operating condition (refer to Table 2), steady-state TMP data registered within the 1- to 2-h operational duration was chosen to compute the reversible fouling rate (rf). This rate was defined as the gradient of the TMP and filtration time data, expressed as:

$$rf = \Delta\mathrm{TMP}/\Delta t \tag{2}$$

The total filtration resistance was determined according to Equation (3):

$$R_\mathrm{t} = R_\mathrm{m} + R_\mathrm{r} + R_\mathrm{irr} \tag{3}$$

Here, R_t and R_m are the total and intrinsic membrane resistances, respectively. While R_r and R_irr are reversible and irreversible fouling resistances, respectively.

Given that it was accepted that all reversible fouling was removed during the relaxation periods, the TMP immediately following relaxation (TMP_0) was attributed to the intrinsic membrane resistance (R_m) and the physically irreversible fouling resistance (R_irr) Equation (4):

$$R_\mathrm{m} + R_\mathrm{irr} = \frac{\mathrm{TMP}_0}{\mu J} \tag{4}$$

Following a similar approach, the TMP variations just before and after relaxation could be attributed to the resistance posed by a physically removable cake layer, i.e., reversible fouling resistance (R_r) Equation (5):

$$R_r = \frac{TMP_1 - TMP_0}{\mu J} \tag{5}$$

where TMP_1 and TMP_0 represent the TMP data immediately before and after the relaxation period.

Equation (4) was employed to calculate the membrane resistance (R_m), subsequently facilitating the straightforward calculation of R_f using Equation (5).

R_{irr} constitutes an irreversible fouling, although a significant portion of this fouling can be removed through chemical cleaning. It should be noted that a portion of this fouling may persist even after chemical cleaning (irrecoverable fouling). For this study, it was assumed that irreversible fouling was solely attributed to SMPs, acknowledging that due to technical limitations, insoluble portion of extracellular polymeric substances (EPSs) could not be monitored and measured. Furthermore, irrecoverable fouling was not considered in this analysis.

3. RESULTS AND DISCUSSION

3.1. Organics and nutrients removal performances

The pilot plant consistently demonstrated efficient treatment performances concerning total COD as well as nitrogen forms removal efficiencies throughout the experimental phases. This observation underscores the robustness of AeCMBR systems when operating under salinity conditions in the short term. As depicted in Figure 2(a), during the initial phase where no salt was introduced, the COD removal efficiency reached 92%. Likewise, in the second phase (5 g NaCl/L), the average COD reduction reached 91%. This outcome suggests the successful acclimatization of the bacterial community to the moderately saline environment.

However, in the subsequent Phase III (10 g NaCl/L), a notable decline in removal efficiency was observed, plummeting to 75%. Notably, during Phase III, there was a sharp drop in removal efficiency from 93 to 75% between days 32 and 34. This outcome could be attributed to the stress-induced impact on biomass activity resulting from the elevated salt concentration (Mannina *et al.* 2016). This fluctuation could be more attributed to the bacterial community realigning itself to fully adapt to the substantial shock load. Following this period, the removal efficiency gradually increased, ultimately reaching 96% on the final day of Phase III. The same trend was observed during Phases IV and V.

Figure 2(b) also provides insight into the biological COD removal efficiency. In Phase I, the biological COD removal efficiency averaged at approximately 77%. However, with the escalation in salinity to 5 and 10 g NaCl/L (Phase I and II), a noticeable decline in removal efficiency was evident, reaching its lowest value at 58 and 56%, respectively. This decrease

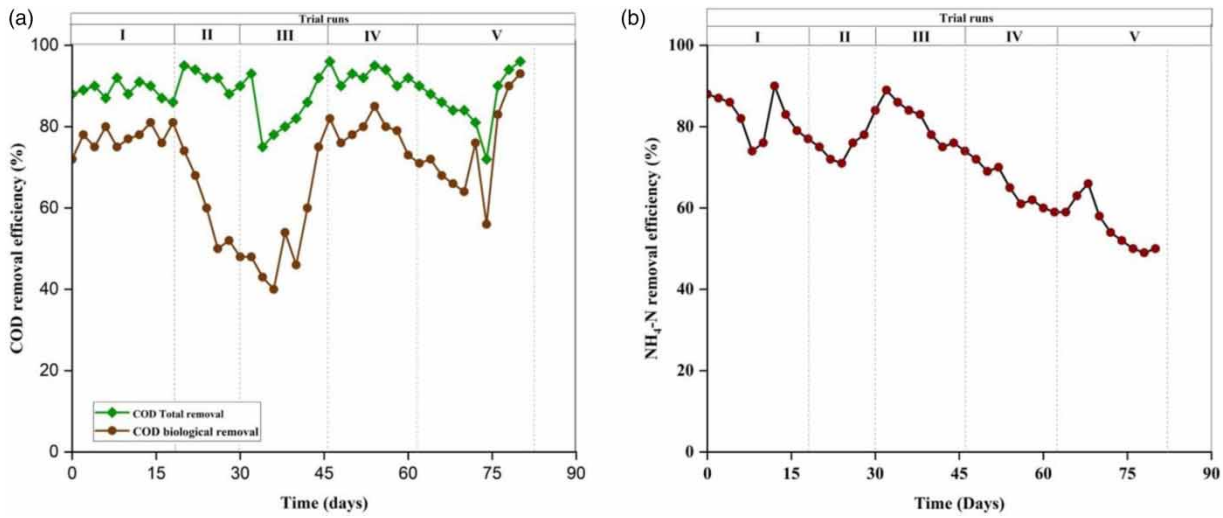

Figure 2 | The biological performance related to COD removal efficiency (a) and NH_4-N removal efficiency (b).

could probably be ascribed to the initial inhibitory impact of salinity on the biomass, affecting metabolic activity and resulting in cell plasmolysis (Johir *et al.* 2013). This behavior is likely because the impact of increased salinity on nitrifiers is more significant at salt concentrations up to 10 g/L. Therefore, a salt concentration of 10 g NaCl/ L could serve as a threshold for significant stress effects, even when the biomass has acclimated. Similar findings have been reported in previous studies (Moussa *et al.* 2006; Johir *et al.* 2013; Mannina *et al.* 2016). An earlier study also reported that the loss of nitrification activity was significantly greater within this concentration range (10 g NaCl/L) (Panswad & Anan 1999). Specifically, during Phases IV and V (15 and 20 NaCl/L), except for a decline on day 75, which we attribute to bacterial re-synchronization, there was a consistent increase in the biological COD removal. This pattern emerged as the feed salt level in the pilot plant remained constant. These results agree with other previous studies (Yogalakshmi & Joseph 2010; Jang *et al.* 2013; Johir *et al.* 2013) and underscore the ability of biomass to facilitate efficient carbon removal, even in the presence of high-salinity concentrations and extended loading times (Wang *et al.* 2023).

The NH_4-N removal data for the AeCMBR is presented in Figure 2(b). During the initial phase, NH_4-N removal exceeded 82%. As the salt concentration increased from 0 to 5 g NaCl/L, the ammonia removal efficiency declined from an average of 82 to 76%. However, in Phase III (10 g NaCl/L), we responded by increasing the oxygenation rate from 700–1,000 NL/h to 1,000–1,500 NL/h. This adjustment aimed to counteract the inhibition of metabolic activity and promote the growth rate of nitrifying bacteria. Consequently, there was a gradual improvement in ammonia removal efficiency, which, at the very least, facilitated the achievement of favored-state nitrification, with an average removal efficiency of 80%. In contrast, during Phases IV and V, a significant decrease in ammonia removal was observed despite the increased oxygenation flow, reaching 66 and 55%, respectively. This trend aligns with the findings of several previous studies, confirming that the addition of salt has an adverse impact on AOB (*Nitrosomonas* group) and NOB (*Nitrobacter*) (Jang *et al.* 2013; Mannina *et al.* 2016; Wang *et al.* 2023). For instance, Ye *et al.* (2009) noted a sharp decrease in the number of NOBs when salinity exceeded 1% (10 g/L) and reported NOB presence of less than 1% when salinity exceeded 2% (w/v) or 20 g/L (Ye *et al.* 2009). Similarly, Yogalakshmi & Joseph (2010) found that nitrite and ammonia oxidants are highly sensitive to both short-term and long-term salt stress, leading to reduced nitrogen removal (Yogalakshmi & Joseph 2010).

Furthermore, Chen *et al.* (2003) reported the disappearance of *Nitrobacter* when chloride concentration exceeded 18 g/L (Chen *et al.* 2003). Considering these results, it can be inferred that there is an additional threshold, and the salt tolerance capacity of nitrifiers may extend to 15 g/L of NaCl when adequate aeration conditions are met. To enhance the interpretation of the kinetic behavior of autotrophic and heterotrophic bacteria participating in this process, it would be highly beneficial to conduct respirometric studies and tests. Such tests serve as an ideal tool for gaining deeper insights for such an operation.

3.2. Variation of MLSS, MLVSS, SMP in the AeCMBR

Figure 3 illustrates the variations in MLSS and MLVSS concentrations during the AeCMBR operation. In the initial operational phase, the average concentrations of MLSS and MLVSS were 2,360 mg/L and 1,847 mg/L, respectively. Despite

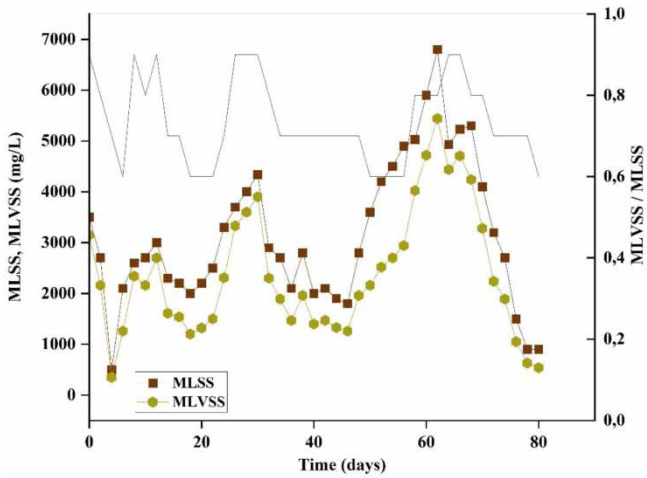

Figure 3 | Variations of MLSS and MLVSS concentrations in AeCMBR.

an adequate HRT of 20 h and an infinite SRT, this phase exhibited a gradual decline followed by a subsequent increase, resulting in the lowest MLSS and MLVSS quantities observed throughout the operation, namely, 500 and 350 mg/L, respectively. In the second phase, with an average conductivity of 2,260 μS/cm, concentrations experienced slight fluctuations and stabilized around 3,500 mg/L for MLSS and 1,500 mg/L for MLVSS. Eventually, they gradually rose to 4,340 and 3,900 mg/L, respectively, by the phase's end.

During the third phase, the introduction of 10 g NaCl/L into the influent significantly reduced MLSS and MLVSS concentrations in the AeCMBR to 1,800 and 1,260 mg/L, respectively. Upon further increasing the NaCl concentration in the influent to 15 g NaCl/L, a substantial rise in MLSS and MLVSS was observed. This phase marked the peak production of MLSS and MLVSS throughout the operation, reaching concentrations of 6,800 mg/L for MLSS and 5,440 mg/L for MLVSS. This increase can be attributed to the abundant organic load in the wastewater and inadequate sedimentation conditions during this phase. It is worth noting that the influent COD averaged 716 mg/L, and the oxygenation rate was sufficient to support bacterial growth. In Phase V (20 gNaCl/L), the additional salt dose led to a further reduction in MLSS and MLVSS concentrations, averaging 3,100 and 2,500 mg/L, respectively. The decrease in MLSS and MLVSS concentration implies that biomass loss occurred as a result of mortality and washout processes. The detrimental impact of salt addition was most pronounced in the AeCMBR, where concentrations dropped to 900 mg/L for MLSS and 540 mg/L for MLVSS. Similar negative effects of salt addition on AeMBRs have also been documented by previous studies (Song *et al.* 2016; Teng *et al.* 2020; Cifuentes-Cabezas *et al.* 2022).

The MLVSS/MLSS ratios typically decreased under high salt concentrations. Interestingly, during the experimental phases, the MLSS:MLVSS ratio exhibited fluctuations, ranging from low to high, even when transitioning from one NaCl dosage to a higher level. Specifically, the average MLVSS/MLSS ratios at salt concentrations of 0, 5, 10, 15, and 20 g NaCl/L were recorded as 0.76, 0.76, 0.71, 0.68, and 0.75, respectively. This decline in the MLVSS/MLSS ratio suggests the accumulation of more inorganic constituents within the system. Throughout the experiment, the MLSS:MLVSS ratio displayed variations within the range of 0.6–0.9, with an average value of approximately 0.7, this ratio is generally considered indicative of stable treatment within the bioreactors.

SMP is a critical indicator in MBR operations, as these concentrations are the primary precursors of clogging phenomena, where about 26–52% of the total resistance can be attributed to the soluble fraction of sludge (Wisniewski & Grasmick 1998; Bouhabila *et al.* 2001). Table 3 provides an overview of SMP production across the experimental phases within the two compartments, the anoxic and aerobic reactors. SMP concentrations did not vary appreciably throughout the operation of the pilot. In the initial phase, both the anoxic and aerobic reactors exhibited substantial SMP concentrations, measuring at 263.53 and 268.2087 mg/L, respectively. Moving to the second phase, the SMP concentration in the anoxic reactor notably decreased to 38.7 mg/L, while the aerobic reactor maintained a concentration of 173.045 mg/L. This decrease in the anoxic reactor can be attributed to the low F/M ratio (0.073 kgBOD/kgVSS/day) observed during Phases II and V. This condition which could lead the microorganisms to use the SMPs released as a substrate, and this agrees with the results of previous research. For instance, Mannina *et al.* (2016) found that under low F/M ratios of 0.085 kg BOD/kg VSS/day, SMP production nearly ceases due to the deterioration of anoxic conditions (Mannina *et al.* 2016). The third phase showed a considerable increase in SMP levels, averaging 449.21 mg/L across both reactors.

Existing literature suggests that higher salinity levels can increase SMP production, primarily in the form of carbohydrate fractions, which might contribute to the development of a gel layer on the membrane surface (Ramesh *et al.* 2007). Phase IV registered the highest SMP concentration during the entire experiment, reaching a total of 570.482 mg/L. The hypertonic conditions induced by salinity during this phase can result in plasmolysis (Kincannon & Gaudy 1968) and exacerbate cell lysis. The release of intracellular constituents after cell lysis likely contributed to the increased SMP content (Luo *et al.* 2016). In the final phase, the average SMP concentration across both reactors remained below 201.20 mg/L. The challenges in

Table 3 | Variation of SMPs in the anoxic and aerobic reactors

	Phase I		Phase II		Phase III		Phase IV		Phase V	
Phase	Anoxic	Aerobic	Anoxic	Aerobic	Anoxic	Aerobic	Anoxic	Aerobic	Anoxic	Aerobic
Day	0–18		19–30		31–46		47–62		63–80	
SMPs (mg/L)	263.53	268.21	38.70	173.04	295.96	153.25	265.39	305.09	83.93	117.27

maintaining anoxic metabolisms, which constrained the anoxic growth of heterotrophic biomass in the anoxic reactor, continued to impact SMP production.

Overall, SMP concentrations showed relative stability throughout the AeCMBR pilot's operation, with no clear correlation observed with increased salt concentration. This observation contradicts with other previous studies (Ramesh *et al.* 2007; Jang *et al.* 2013; Johir *et al.* 2013). The contrast in outcomes is primarily attributed to differences in membrane properties and the gradual temporal dosing of salinity.

3.3. Sludge properties

Elevated salt concentrations result in increased water density, potentially affecting settling characteristics (Moussa *et al.* 2006) .The sludge volume index (SVI), which provides an indirect measure of biomass settling properties, was consistently monitored throughout all experimental phases, employing a systematic approach with a 2-day interval (Figure 4). The measurement procedure initiated with the collection of a representative mixed liquor sample from the aeration tank. After allowing the sample to settle undisturbed for 30 min, the settled sludge volume (SSV) was meticulously quantified in milliliters (mL). Concurrently, the concentration of MLSS was determined through laboratory filtration and analysis. These values were subsequently applied to the SVI formula: SVI = (SSV, mL)/(MLSS, mg/L).

The derived SVI values offered critical insights into sludge settling characteristics. Throughout the experimental Phases (I, II, III, IV, V), the SVI values were as follows: 82, 90, 75, and 100.82 mL/g, respectively. The SVI gradually increased from 82 mL/g (Phase I) to 90 mL/g (Phase II). However, it decreased from 90 to 75 mL/g between Phases II and III. This decrease could be attributed to the rapid adaptation to salinity, primarily due to the poor settling properties of small aggregates or dispersed organisms that have been evacuated from the reactor. Subsequently, the SVI increased to 100 mL/g (Phase IV) and then stabilized at 82 mL/g (Phase V), representing a reduction in SVI that was slightly greater than the transition from Phase I to Phase II. According to Moussa *et al.* (2006), increased salinity levels, and the consequent rise in water density, favor the removal of lighter flocs while denser flocs remain in the reactor, leading to a decrease in the SVI (Moussa *et al.* 2006).

In general, during our experiment, SVI exhibited fluctuations in response to increasing salinity while still demonstrating acceptable sedimentation. This finding contradicts the results of several studies, including those by Campos *et al.* (2002) and Moussa *et al.* (2006), who observed a decrease in SVI with rising salt concentrations (Campos *et al.* 2002; Moussa *et al.* 2006). On the other hand, Bassin *et al.* (2012) noted that increasing salt concentrations induce physical changes in aggregates and observed an initial increase in SVI following salt concentration increase (Bassin *et al.* 2012).

3.4. Effect of salinity on the membrane fouling

To illustrate how membrane filtration responds to salinity stresses, TMP was continuously monitored at a constant flux of 20 LMH. Since a peristaltic pump produced the permeate and the pressure in the retentate remained unchanged, TMP naturally increased due to fouling, resulting in a decline in permeate pressure.

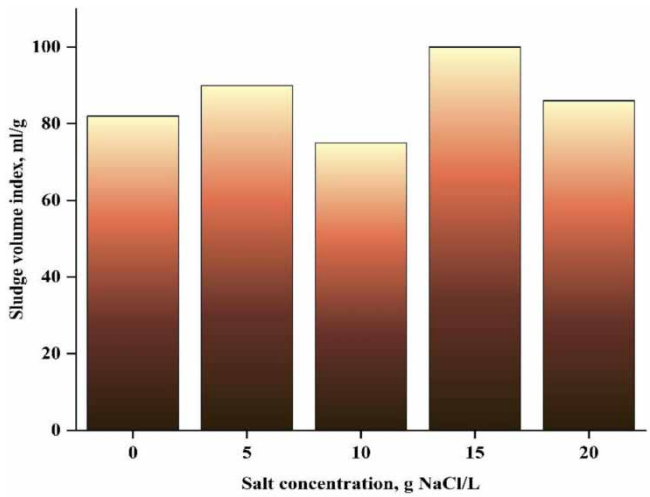

Figure 4 | SVI measurements under varying salt concentrations.

Figure 5 displays the TMP profiles over time throughout all operational phases. In the initial Phase, where no salt was added, TMP approached the critical flux threshold of 2.5 bar after 15 days of operation, prompting chemical cleaning. The results indicated that fouling propensity increased significantly even before salt concentrations were introduced. The fouling rate during the final week of the first phase reached 0.13 bar/day. This abrupt TMP rise can be well explained by the concept of local critical flux (Ognier *et al.* 2004). Consequently, under subcritical membrane filtration (when the permeation flux value is below the critical flux value), a gel layer formed on the membrane, followed by the rapid formation of a cake layer (Wang & Wu 2009), suggesting that the flux (20 LMH) was higher and accelerated fouling. Emphasizing, that we relied on the intrinsic resistance of the membrane given by the manufacturer, and that the pilot was operated well just before our investigation, it may be that the membrane was not completely cleaned during start-up. During Phase II (5 g NaCl/L), the initial TMP increase was relatively slow, with a fouling rate of approximately 0.1 ± 0.05 bar/day during the first week. This was likely because the biomass could adapt more readily to modest increases in salt concentration, thereby having a lesser impact on biomass detachment. Subsequently, after the first week, TMP gradually increased at a rate of roughly 0.3 bar/day.

During Phases I and II, the flux in the AeCMBR was maintained at 20 LMH but was subsequently reduced to 15 LMH for the rest of the operation, as indicated in Table 2. After this flux reduction on day 31, the pilot plant operated without the need for chemical cleaning for a continuous 45-day period. During Phase III, characterized by a salinity increase to 10 g NaCl/L, TMP irregularly increased but did not lead to significant membrane fouling, averaging at 1.34 bar. The gradual TMP increase observed during this Phase can be attributed to the prolonged accumulation of a gel layer and cake on the membrane surface under subcritical flux conditions. This suggests that the filtration cycle strategy was effective, as indicated by the TMP decrease between days 35 and 45. In Phase IV, following day 55, TMP steadily increased, even after the flux was reduced to 15 LMH, reaching 2.47 bar by day 60 when chemical cleaning was performed. High salt concentrations can also elevate viscosity and intensify fouling by forming a denser cake layer, as reported by Lay *et al.* (2010). Phase V, involving an increase in salt concentration from 15 to 20 g NaCl/L, did not exhibit sudden increases in membrane fouling due to biomass detachment (Lay *et al.* 2010). Beyond day 60, TMP remained stable at low levels for the subsequent 20 days, with reversible fouling rates measured at 5 mbar/h.

The series resistance model was employed to determine the contribution of each resistance to membrane fouling (Figure 6). Reversible cake deposition (R_C) emerged as the dominant fouling mechanism throughout the entire operational period. In the initial phase, the total resistance reached 1.8×10^{13} 1/m, but after chemical cleaning, it averaged around 0.5×10^{13} 1/m.

A noticeable reduction in R_C was observed alongside an increase in salt concentration when transitioning from 5 to 10 to 15 g NaCl/L, with corresponding reductions of 88, 83, and 72%, respectively. Conversely, R_{irrev} increased from 4 to 7% when shifting from Phase II (5 g NaCl/L) to Phase III (10 g NaCl/L), then spiked to 20% during Phase IV (15 g NaCl/L). These results clearly indicate that R_{irrev} played a significant role in elevating TMP, resulting in a substantial loss of permeability,

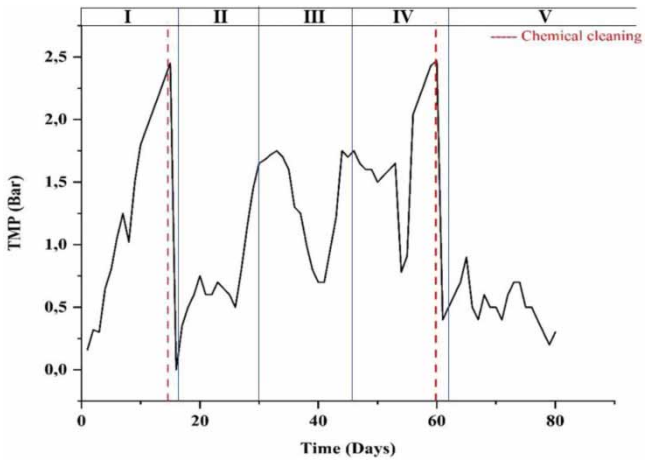

Figure 5 | TMP temporal variation in AeCMBR.

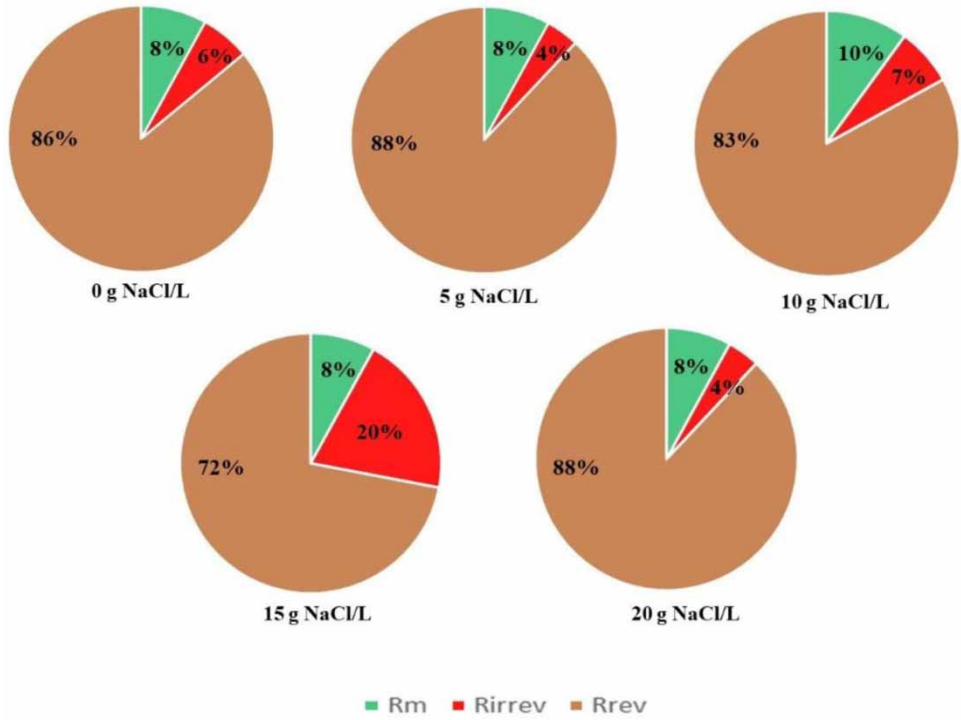

Figure 6 | Resistance fractions at various salt loadings (R_m: membrane resistance, R_{irrev}: irreversible resistance, and R_{rev}: reversible resistance).

particularly at salt concentrations of 15 g NaCl/L. Chemical cleaning was implemented on day 60, targeting R_{irrev}, which accounted for 20% of the total resistance. This was likely a response to significant SMP accumulation in the floc during prior phases. Interestingly, right after the cleaning et just before the addition of 20 g NaCl/L, nearly all fouling seemed to be removed, favoring the reduction of the Rirrev to 4%. This might seem counterintuitive. During Phase VI (20 g NaCl/L), the SMP value in the mixed liquor was the lowest observed throughout the process, at 117.27 mg/L. This decline from days 60 to 80 was probably attributed to the stable characteristics of the sludge and the diluted nature of the fed municipal wastewater. The high salinity did not impact sludge characteristics, contributing to a stable hydrophobicity of the cake layer, resulting in an irreversible strength reduction. After the chemical cleaning on day 60, the total resistance averaged approximately 0.3×10^{13} L/m until the end of the operation. Similar findings were reported in a study by Mannina *et al.* (2016), wherein they observed a decrease in irreversible cake resistance (RC_{irrev}) as the salt concentration increased from 0 to 10 g of NaCl/L (Mannina *et al.* 2016). These findings align with prior research, which demonstrated that pollutants exhibit minimal transfer from the membrane surface to the pores under gradual changes in salinity conditions (Di Trapani *et al.* 2014).

3.5. Applicability of the pilot roject

The results of our survey of an AeCMBR pilot plant treating wastewater with rising salinity have significant implications for future pilot projects, especially in the treatment of fish canning wastewater. The consistent fouling of the membrane due to reversible cake deposition highlights the challenges associated with salinity in wastewater from such industrial processes. Future projects in fish canning wastewater treatment could leverage the insights gained from this study to optimize MBR systems, ensuring effective and sustainable treatment even in the presence of varying salinity levels. Considering the environmental conditions of remote regions, such as the Saharan region dominated by invasion and saline agriculture, the study provides valuable insights. The graduated salinity tests revealing no consistent impact on treatment effectiveness suggest that the AeCMBR technology may offer resilience in diverse and challenging environmental settings. The capability of nitrifiers to handle up to 15 g/L NaCl with proper aeration is particularly promising for regions with high salinity. This technology

could prove beneficial in addressing wastewater challenges in remote areas where water scarcity and the need for effective treatment are critical. The applicability of this pilot extends beyond specific industries or regions. The study emphasizes the importance of thorough homogenization in municipal wastewater treatment, showcasing the adaptability of AeCMBR technology to complex and diverse wastewater compositions.

In conclusion, the AeCMBR pilot project emerges as a versatile and resilient solution for wastewater treatment, poised for applications in various industries and harsh environmental conditions. Its advantages over similar technologies position it as a compelling choice for decision-makers and practitioners seeking efficient and sustainable wastewater treatment options.

4. CONCLUSION

The study investigated the immediate consequences of a substantial increase in salinity in a pilot-scale AeCMBR treating municipal wastewater. Notably, a considerable proportion of COD was effectively removed, achieving a 90% efficiency rate. However, the removal of NH_4-N was significantly impacted, dropping from 82 to 55%. This performance could be enhanced through extended acclimatization periods. Metrics such as MLSS, MLVSS, and the MLVSS/MLSS ratio exhibited fluctuations with increasing salinity levels. The gradual rise in salt concentration appeared to improve the settling characteristics of the sludge. Unexpectedly, salt stress did not directly influence the release of SMPs, which, particularly at concentrations of 15 g NaCl/L, became attached and were retained by a gel or cake layer formed on the membrane surface. This phenomenon increased filtration resistance and elevated the TMP, despite a reduced flux rate from 20 to 15 LMH. The primary fouling mechanism observed was the reversible deposition of a cake layer on the membrane surface. In summary, this study offers a comprehensive insight into the immediate impacts of salinity on the extended operation of AeCMBR, enhancing our understanding of associated phenomena and facilitating the development of more resilient MBR-based strategies to tackle the growing problem of increased salinity in urban wastewaters.

DATA AVAILABILITY STATEMENT

All relevant data are included in the paper or its Supplementary Information.

CONFLICT OF INTEREST

The authors declare there is no conflict.

REFERENCES

Amin, M. M., Khiadani, M. H., Fatehizadeh, A. & Taheri, E. 2014 Validation of linear and non-linear kinetic modeling of saline wastewater treatment by sequencing batch reactor with adapted and non-adapted consortiums. *Desalination* **344**, 228–235.

APHA 2005 'WEF, 2005', Standard methods for the examination of water and wastewater, **21**, pp. 258–259.

Aryanti, P. T. P., Subroto, E., Mangindaan, D., Widiasa, I. N., & Wenten, I. G. 2020 Semi-industrial high-temperature ceramic membrane clarification during starch hydrolysis. *Journal of Food Engineering* **274**, 109844.

Ayyoub, H., Elmoutez, S., El-Ghzizel, S., Elmidaoui, A. & Taky, M. 2023 Aerobic treatment of fish canning wastewater using a pilot-scale external membrane bioreactor. *Results in Engineering* **17**, 101019.

Bassin, J. P., Kleerebezem, R., Muyzer, G., Rosado, A. S., Van Loosdrecht, M. C. M. & Dezotti, M. 2012 Effect of different salt adaptation strategies on the microbial diversity, activity, and settling of nitrifying sludge in sequencing batch reactors. *Applied Microbiology and Biotechnology* **93**, 1281–1294.

Bouhabila, E. H., Aï̈m, R. B. & Buisson, H. 2001 Fouling characterisation in membrane bioreactors. *Separation and Purification Technology* **22**, 123–132.

Campos, J. L., Mosquera-Corral, A., Sanchez, M., Méndez, R. & Lema, J. M. 2002 Nitrification in saline wastewater with high ammonia concentration in an activated sludge unit. *Water Research* **36** (10), 2555–2560.

Capodici, M., Cosenza, A., Di Bella, G., Di Trapani, D., Viviani, G. & Mannina, G. 2020 High salinity wastewater treatment by membrane bioreactors. *Current Developments in Biotechnology and Bioengineering* 177–204.

Chen, R. D. & LaPara, T. M. 2008 Enrichment of dense nitrifying bacterial communities in membrane-coupled bioreactors. *Process Biochemistry* **43** (1), 33–41.

Chen, G.-H., Wong, M.-T., Okabe, S. & Watanabe, Y. 2003 Dynamic response of nitrifying activated sludge batch culture to increased chloride concentration. *Water Research* **37** (13), 3125–3135.

Cifuentes-Cabezas, M., Vincent-Vela, M. C., Mendoza-Roca, J. A. & Álvarez-Blanco, S. 2022 Use of ultrafiltration ceramic membranes as a first step treatment for olive oil washing wastewater. *Food and Bioproducts Processing* **135**, 60–73.

Di Trapani, D., Di Bella, G., Mannina, G., Torregrossa, M. & Viviani, G. 2014 Comparison between moving bed-membrane bioreactor (MB-MBR) and membrane bioreactor (MBR) systems: influence of wastewater salinity variation. *Bioresource Technology* **162**, 60–69.

Elfilali, N., Elazhar, F., Dhiba, D., Elmidaoui, A. & Taky, M. 2022 Performances of various hybrids systems coagulation–ultrafiltration/nanofiltration-reverse osmosis in the treatment of stabilized landfill leachate. *Desalination and Water Treatment* **257**, 55–63.

El-Ghzizel, S., Zeggar, H., Tahaikt, M., Tiyal, F., Elmidaoui, A. & Taky, M. 2020 Nanofiltration process combined with electrochemical disinfection for drinking water production: Feasibility study and optimization. *Journal of Water Process Engineering* **36**, 101225.

Elmoutez, S., Abushaban, A., Necibi, M. C., Sillanpää, M., Liu, J., Dhiba, D., Chehbouni, A. & Taky, M. 2023 Design and operational aspects of anaerobic membrane bioreactor for efficient wastewater treatment and biogas production. *Environmental Challenges* **10**, 100671.

Jang, D., Hwang, Y., Shin, H. & Lee, W. 2013 Effects of salinity on the characteristics of biomass and membrane fouling in membrane bioreactors. *Bioresource Technology* **141**, 50–56.

Johir, M. A. H., Vigneswaran, S., Kandasamy, J., BenAim, R. & Grasmick, A 2013 Effect of salt concentration on membrane bioreactor (MBR) performances: Detailed organic characterization. *Desalination* **322**, 13–20.

Judd, S. 2010 *The MBR Book: Principles and Applications of Membrane Bioreactors for Water and Wastewater Treatment*. Elsevier, Amsterdam.

Kincannon, D. F. & Gaudy Jr., A. F. 1968 Response of biological waste treatment systems to changes in salt concentrations. *Biotechnology and Bioengineering* **10** (4), 483–496.

Lay, W. C. L., Liu, Y. & Fane, A. G. 2010 Impacts of salinity on the performance of high retention membrane bioreactors for water reclamation: A review. *Water Research* **44** (1), 21–40.

Lefebvre, O., Quentin, S., Torrijos, M., Godon, J.-J., Delgenes, J. P. & Moletta, R. 2007 Impact of increasing NaCl concentrations on the performance and community composition of two anaerobic reactors. *Applied Microbiology and Biotechnology* **75**, 61–69.

Luo, W., Hai, F. I., Kang, J., Price, W. E., Guo, W., Ngo, H. H., Yamamoto, K. & Nghiem, L. D. 2015 Effects of salinity build-up on biomass characteristics and trace organic chemical removal: Implications on the development of high retention membrane bioreactors. *Bioresource Technology* **177**, 274–281.

Luo, W., Phan, H. V, Hai, F. I., Price, W. E., Guo, W., Ngo, H. H., Yamamoto, K. & Nghiem, L. D. 2016 Effects of salinity build-up on the performance and bacterial community structure of a membrane bioreactor. *Bioresource Technology* **200**, 305–310.

Luo, G., Wang, Z., Li, Y., Li, J. & Li, A.-M. 2019 Salinity stresses make a difference in the start-up of membrane bioreactor: Performance, microbial community and membrane fouling. *Bioprocess and Biosystems Engineering* **42**, 445–454.

Mannina, G., Capodici, M., Cosenza, A., Di Trapani, D. & Viviani, G. 2016 Sequential batch membrane bio-reactor for wastewater treatment: The effect of increased salinity. *Bioresource Technology* **209**, 205–212.

Moussa, M. S., Sumanasekera, D. U., Ibrahim, S. H., Lubberding, H. J., Hooijmans, C. M., Gijzen, H. J. & Van Loosdrecht, M. C. M. 2006 Long term effects of salt on activity, population structure and floc characteristics in enriched bacterial cultures of nitrifiers. *Water Research* **40** (7), 1377–1388.

Ni, B.-J., Rittmann, B. E. & Yu, H.-Q. 2011 Soluble microbial products and their implications in mixed culture biotechnology. *Trends in Biotechnology* **29** (9), 454–463.

Ognier, S., Wisniewski, C. & Grasmick, A. 2004 Membrane bioreactor fouling in sub-critical filtration conditions: A local critical flux concept. *Journal of Membrane Science* **229** (1–2), 171–177.

Panswad, T. & Anan, C. 1999 Impact of high chloride wastewater on an anaerobic/anoxic/aerobic process with and without inoculation of chloride acclimated seeds. *Water Research* **33** (5), 1165–1172.

Ramesh, A., Lee, D. J. & Lai, J. Y. 2007 Membrane biofouling by extracellular polymeric substances or soluble microbial products from membrane bioreactor sludge. *Applied Microbiology and Biotechnology* **74** (3), 699–707.

Song, X., McDonald, J., Price, W. E., Khan, S. J., Hai, F. I., Ngo, H. H., Guo, W. & Nghiem, L. D. 2016 Effects of salinity build-up on the performance of an anaerobic membrane bioreactor regarding basic water quality parameters and removal of trace organic contaminants. *Bioresource Technology* **216**, 399–405.

Tan, X., Acquah, I., Liu, H., Li, W. & Tan, S. 2019 A critical review on saline wastewater treatment by membrane bioreactor (MBR) from a microbial perspective. *Chemosphere* **220**, 1150–1162.

Teng, J., Shen, L., Xu, Y., Chen, Y., Wu, X.-L., He, Y., Chen, J. & Lin, H. 2020 Effects of molecular weight distribution of soluble microbial products (SMPs) on membrane fouling in a membrane bioreactor (MBR): Novel mechanistic insights. *Chemosphere* **248**, 126013.

Uygur, A. 2006 Specific nutrient removal rates in saline wastewater treatment using sequencing batch reactor. *Process Biochemistry* **41** (1), 61–66.

Wang, Z. & Wu, Z. 2009 A review of membrane fouling in MBRs: Characteristics and role of sludge cake formed on membrane surfaces. *Separation Science and Technology* **44** (15), 3571–3596.

Wang, Z. C., Gao, M. C., Ren, Y., Wang, Z., She, Z. L., Jin, C. J., Chang, Q. B., Sun, C. Q., Zhang, J. & Yang, N. 2015 Effect of hydraulic retention time on performance of an anoxic–aerobic sequencing batch reactor treating saline wastewater. *International Journal of Environmental Science and Technology* **12**, 2043–2054.

Wang, K., Zhang, H., Shen, Y., Li, J., Zhou, W., Song, H., Liu, M. & Wang, H. 2023 Impact of salinity on anaerobic ceramic membrane bioreactor for textile wastewater treatment: Process performance, membrane fouling and machine learning models. *Journal of Environmental Management* **345**, 118717.

Wef, A. A. no date Standard Methods. 2005. *Standard Methods*, 3030, p. 825.
Wenten, I. G., Khoiruddin, K., Aryanti, P. T. P. & Hakim, A. N. 2016 Scale-up strategies for membrane-based desalination processes: A review. *Journal of Membrane Science and Research* **2** (2), 42–58.
Wenten, I. G., Friatnasary, D. L., Khoiruddin, K., Setiadi, T. & Boopathy, R. 2020 Extractive membrane bioreactor (EMBR): Recent advances and applications. *Bioresource Technology* **297**, 122424.
Wintgens, T., Melin, T., Schäfer, A., Khan, S., Muston, M., Bixio, D. & Thoeye, C. 2005 The role of membrane processes in municipal wastewater reclamation and reuse. *Desalination* **178** (1–3), 1–11.
Wisniewski, C. & Grasmick, A. 1998 Floc size distribution in a membrane bioreactor and consequences for membrane fouling. *Colloids and Surfaces A: Physicochemical and Engineering Aspects* **138** (2–3), 403–411.
Ye, L., Peng, C., Tang, B., Wang, S., Zhao, K. & Peng, Y. 2009 Determination effect of influent salinity and inhibition time on partial nitrification in a sequencing batch reactor treating saline sewage. *Desalination* **246** (1–3), 556–566.
Yogalakshmi, K. N. & Joseph, K. 2010 Effect of transient sodium chloride shock loads on the performance of submerged membrane bioreactor. *Bioresource Technology* **101** (18), 7054–7061.
Yu, T., Li, D., Qi, R., Li, S., Xu, S. & Yang, M. 2011 Structure and dynamics of nitrifier populations in a full-scale submerged membrane bioreactor during start-up. *Applied Microbiology and Biotechnology* **90**, 369–376.
Zaita, M., Addara, F. Z., Elfilalia, N., Tahaikta, M., Elmidaouia, A. & Takya, M. 2022 Analysis and optimization of operating conditions on ultrafiltration of landfill leachate using a response surface methodological approach. *Desalination and Water Treatment* **257**, 64–75.
Zhang, X., Gao, J., Zhao, F., Zhao, Y. & Li, Z. 2014 Characterization of a salt-tolerant bacterium *Bacillus sp*. from a membrane bioreactor for saline wastewater treatment. *Journal of Environmental Sciences* **26** (6), 1369–1374.

First received 8 December 2023; accepted in revised form 16 February 2024. Available online 28 February 2024